Publishing House
AKAPIT

COMPUTER METHODS IN MATERIALS SCIENCE
Informatyka w Technologii Materiałów

Vol. 17, 2017, No. 3

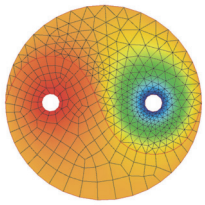

MODELLING THE EFFECT OF PHASE TRANSFORMATIONS ON COOLING RATE DURING QUENCHING IN NUCLEAR FORGINGS USING EFFECTIVE HEAT CAPACITY

M.P. HOWSON[1*], B.P. WYNNE[2], P.S. DAVIES[3], J. TALAMANTES-SILVA[4]

[1] EPSRC Centre for Doctoral Training in Advanced Metallic Systems, Department of Materials Science and Engineering, The University of Sheffield, Mappin St., Sheffield S1 3JD, UK.
[2] Department of Materials Science and Engineering, The University of Sheffield, Mappin St., Sheffield S1 3JD, UK.
[3] Sheffield Forgemasters RD26 Ltd, 286 Brightside Lane, Sheffield S9 2RW, UK
**Corresponding author: mhowson1@sheffield.ac.uk*

Abstract

A modelling methodology based on experimental heat capacity measurements has been used to predict the effects of latent heat formation on cooling rates in a thick sectioned nuclear forging during quenching. Differential scanning calorimetry was used to measure specific heat capacity as a function of temperature (100 - 1000°C) and cooling rate (5 and 70°C/min) that also incorporates the heat energy release during transformations, which is termed the effective specific heat. A user defined routine then incorporated this data into a finite element model of a full scale heat treatment trial forging that had section thicknesses of 200.5 and 331mm. Excellent agreement with thermocouple data, taken from key test locations, was obtained, particularly at 0.25 and 0.5 thickness. However, some deviations from thermocouple data was seen that has been attributed to the model assumptions, particularly the method used to represent boundary conditions.

Key words: Quenching; Reactor Pressure Vessel; Finite Element Modeling; Differential Scanning Colorimetry; Latent Heat

1. INTRODUCTION

Pressure vessels within the primary circuit of light water nuclear reactors, such as steam generators, pressurisers and reactor vessels, are generally constructed from multiple high integrity, thick sectioned steel forgings. The mechanical properties of each forging must be sufficient to ensure structural integrity and reliability over the operational lifetime of the reactor as well as offer a significant safety margin.

Nuclear forgings are almost exclusively manufactured using high strength, low alloy steel grades, such as SA508 grade 3. The accumulated operational and manufacturing experience generated using these materials means there is little impetus to alter tried and tested composition ranges. The industry has therefore focused on the refinement of the manufacturing process in order to optimise mechanical properties. The cost and size of each forging means that full scale optimisation investigations are both costly and impractical. Combining this with the inability to reproduce production scale conditions in the laboratory means process modelling is critical for producing enhancements to current manufacturing routes.

Pressure vessel forgings manufactured in the United Kingdom must adhere to the American Society of Mechanical Engineers (ASME) boiler and Pressure Vessel Code (ASME 2013a). In addition to

ISSN 1641-8581

impact toughness and tensile strength property requirements, the code gives details of a heat treatment for final properties. Known industrially as the quality heat treatment (QHT), this consists of austinitisation, quench and temper processes. The thick section of a nuclear forging means that cooling rates during quenching decrease as a function of distance from the surface, leading to variability in microstructure and mechanical properties (Kim et al., 1997b). For example, Kim et al. (1997a) and Pous-Romero and Bhadeshia (2014) have identified allotromorphic ferrite as being detrimental to impact properties in SA508-3 and therefore, it must be minimised. Computer modelling can be used to identify cooling rates and design heat treatments that avoid ferrite formation in quantities that will result in a forging's failure to meet specification property values.

Modelling efforts must accurately reproduce a range of scientific phenomena that occur when quenching. This includes latent heat produced during phase transformations, which has been shown to have a marked influence on cooling rates in thick sections Haverkamp et al. (1984). For example, both Pan et al. (2002) and Liu et al. (2003) successfully incorporated latent heat into constitutive heat conduction equations, but it is unclear how the data is being used. Liu et al. gave no explanation to the source and form of this data, while Pan et al. states that the internal heat generation can be calculated using Eq. 1 but does not give details regarding the enthalpy values, H in the equation

$$Q_1 = \Delta H \frac{\Delta V}{\Delta t} \tag{1}$$

In a number of small-scale models Hess's law enables the calculation of enthalpy values using a mathematical function (Fernandes et al., 1985). This is reliant on known values of enthalpy and data is available in the literature for the alloy being investigated (Song et al., 2004). However, the thicker section size of nuclear forgings and greater sensitivity of cooling rates to latent heat means it is more appropriate to establish values for the exact chemical composition being utilised, opposed to adopting general values from the literature.

The other terms of eq. 1, i.e. $\Delta V/\Delta t$, are often determined by the Johnson-Mehl-Avrami-Kolmogorov (JAMK) equation (Carlone et al., 2010; Liu et al., 2003; Pan et al., 2002; Woodard et al., 1999). The JMAK equation is reliant on knowledge of the materials critical transformation temperatures, usually obtained from a time, temperature, transformation (TTT) diagram, which requires a considerable amount of experimental work to construct. Thermal property predictive software is therefore used as an alternative to produce TTT diagrams and/or other relevant material data (Al-Bermani et al., 2015; Pola et al., 2013). Previous work by the authors (Howson., 2016) has shown data generated via this software, for SA508-3 steel, cannot always be considered reliable. An alternate modelling approach is therefore required to represent phase transformations in these steels and thick section forgings to ensure the high reliability required from nuclear regulators.

Rammerstorfer et al. (1981) has demonstrated it is possible to simulate the effects of latent heat using a modified value of specific heat capacity. Termed the "effective specific heat" (Cp_{eff}) in a study by Jhajj et al. (2015), it can be determined as a function of cooling rate using differential scanning calorimetry (DSC) (Howson et al., 2016; Krielaart et al., 1996). The objective of the current work is to determine values of Cp_{eff} for the nuclear steel grade SA508-3. Once established these values will be incorporated into a finite element model (FEM), using a user defined subroutine and used to simulate the effects of latent heat, as a function of cooling rate. The simulated cooling curves will then be validated via comparison with production thermocouple data.

2. EXPERIMENTAL PROCEDURE

The material used in this study was nuclear grade SA508-3, composition specification shown in table 1. The test material was taken from a component in the as-forged condition.

DSC Data was acquired using a Netzsch 401 F1 Pegasus DSC analysis machine. Discs, 5 mm in diameter and 0.5 mm thick, were prepared from test material. Cp_{eff} values were determined using the experimental procedure outlined by Krielaart et al. (1996), which requires three separate tests. The first, known as the baseline test, conducts the desired heating and cooling program on two empty cruci-

Table 1. *Chemical composition specification (weight %) for SA508-3, taken from the ASME code (2013a).*

C	Mn	P	S	Si	Ni	Cr	Mo	V	Nb	Cu	Ca	B	Ti	Al	Fe
0.25	1.20-1.50	0.025	0.025	0.4	0.40-1.00	0.25	0.45-0.60	0.05	0.01	0.2	0.015	0.003	0.015	0.025	Rem.

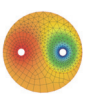

bles. The second, known as the reference, applies the same heating and cooling regime however, a sample of Al_2O_3 with known values of specific heat capacity is placed into one of the crucibles, leaving the other empty. Finally, the sample test repeats that of the reference but with a sample of SA508-3 inserted in a crucible. The crucibles, made of platinum, contained a liner and were enclosed with a platinum lid to minimise heat losses due to radiation and convection. Once a DSC trace had been recorded for the reference and sample the ratio method, eq. 2, was used to calculate Cp_{eff}.

$$Cp_{eff} = \frac{m_{standard}}{m_{sample}} \times \frac{DSC_{sample} - DSC_{base}}{DSC_{Standard} - DSC_{Base}} \times Cp_{Standard} \quad (2)$$

All samples were heated to 30°C and held for 10 minutes to allow the system to equilibrate. This was followed by heating, at a rate of 20°C/min, to 1000°C with a 10 minute hold for austenising. The samples were then cooled at the following cooling rates: 5, 10, 15, 20, 30, 50, 60 and 70°C/min. A schematic representation of this heat treatment program can be seen in figure 1.

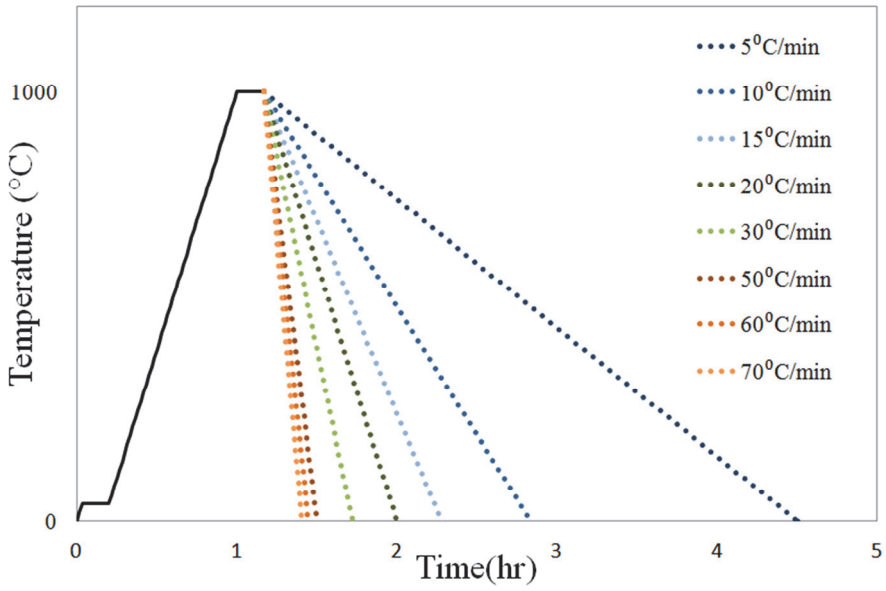

Fig. 1 *Schematic representation of the heating and cooling procedure used in testing*

3. MODEL CONSTRUCTION

The FE model was constructed with commercially available computer software. The geometry represented a hollow nuclear forging used in an experimental heat treatment trial, which was approximately 3400 mm in height with an inner diameter of 1020 mm and a variable outer diameter. The lower end the forging was 315 mm thick whilst the top end was 200.5 mm thick. The mesh generated consisted of 10396 nodes with 37 nodes across the section at the thickest end and 23 nodes at the thinnest. The geometry and applied mesh can be seen in figure 2. Multiple thermocouples, embedded in the forging, were used to validate the constructed model, these were located at 1/4T and 1/2T in both the thin and thick sections, where T represents wall thickness. Thermocouples were also embedded 5mm from the surface of both inner and outer diameters, in both section thicknesses. Similar to the work of Al-Bermani et al. (2015), the time temperature data recorded by the 5 mm deep thermocouples was assigned to the external surfaces of the forging and used to represent heat transfer as a result of quenching. As no material file for SA508-3 was available in the software, a representative material file was chosen and modified with thermal conductivity data as a function of temperature (ASME, 2013b). The user defined route (UDR), discussed later, was used to accommodate phase transformations using Cp_{eff} values. However, as the UDR was recalled at the end of each iteration, the base material file required values of heat capacity without the effects of latent heat in order to calculate temperature change before calling the UDR. These values were determined from the test data. To remove the latent heat of transformation from the heat capacity data, a Matlab script was constructed that linearly interpolated the measured values before and after transformations. This was performed for all cooling rates tested and an average value as function of temperature was calculated. Referred to as the baseline heat capacity, the interpolated data was incorporated into the material file.

The FEM software cannot implement the multiple sets of Cp_{eff} required to represent cooling rate dependant latent heat formation. Therefore, a user defined routine (UDR) was created to access the experimentally generated DSC data. The UDR was written in the programming language FORTRAN 95 and, as previously stated, called at the end of each iteration. Based upon the current temperature of the node and the temperature change for the iteration, the UDR recalculated the new nodal temperature using eq. 3.

$$T_2 = \left(\left(\frac{Cp_{base}}{Cp_{eff}}\right) \times \Delta T\right) + T_1 \qquad (3)$$

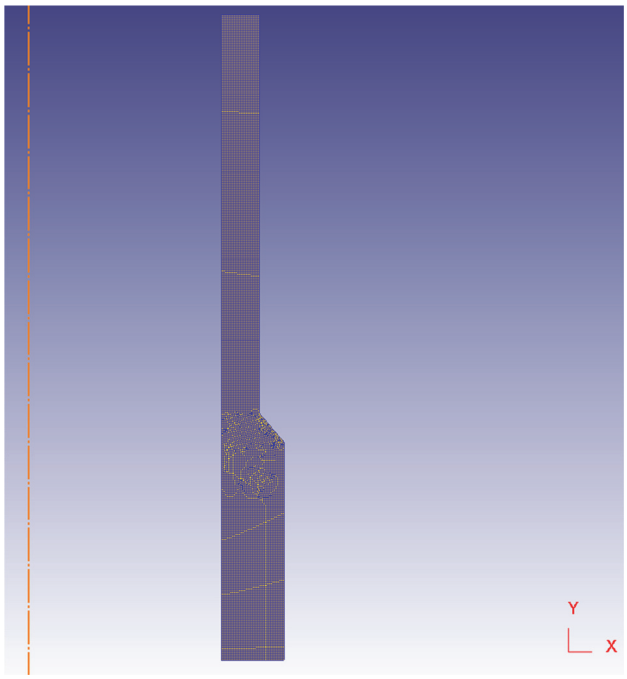

Fig. 2. *Forgings geometry and mesh generated. The line to the left of the image represents the axis symmetry*

Derived from the work of Tewkesbury et al. (2000), T_1 is the nodal temperature and ΔT is the temperature change for the iteration. Cp_{base} is the baseline Cp data and Cp_{eff} is the cooling rate dependent effective specific heat capacity. The UDR chose the correct Cp_{eff} data by recalling the cooling rate of the node between 830 to 800°C. This was calculated and stored to a text file in the initial steps of the model. The temperature window was chosen as it is above the critical transformation temperatures for the steel grade considered, thus, cooling rates can be regarded free from latent heat and approximately constant. To aid the implementation of the model and improve accuracy, the experimental data was interpolated and stored in discrete data sets at cooling rate intervals of 1°C/min. The model was run for 2000 iterations with a maximum time step of 10s and a maximum temperature change of 5°C.

4. RESULTS AND DISCUSSION

Cp_{eff} values for all cooling rates can be seen in figure 3. Transformation start and finish temperatures, with their associated cooling rates, are compared with a continuous cooling transformation (CCT) diagram, which was adapted from Suzuki et al. (2001). The results have been adjusted so that the cooling rates can be considered the axis for the Cp_{eff}. The deviations in Cp, represents the latent heat emitted during phase changes. Two transformations can be seen for most cooling rates and the magnitude of the latent heat response is rate dependent. Cooling rates between 5°C and 15°C/min demonstrate a large latent heat response between 709°C-779°C, which is most likely to be associated with the transformation of austenite to ferrite. Conversely cooling rates in the range of 20°C-70°C/min, see a greater latent heat formation in the second transformation between 341°C-585°C, which is likely to be the result of Bainite formation.

Examination of the test results revealed variations in cooling rate at lower temperatures, this represents a loss of cooling control meaning cooling rates could no longer be considered as constant. However, this occurred after all transformations were completed for the experimentally designated cooling rates of 5°C /min to 20°C /min and, was therefore considered insignificant. For 30°C/min test however, the deviation begins at approximately 460°C, which is during the second transformation. Furthermore, the designated cooling rates 50, 60 and 70°C/min showed non constant cooling rates throughout the experimentation. The loss of control demonstrates the limitation of the equipment in its current configuration, if constant cooling rates to lower temperatures and faster cooling rates is required, additional cooling equipment is needed.

Figure 3 shows that the transformation start temperatures are in general agreement with Suzuki's CCT diagram and, as previously stated, that the first transformation is associated with ferrite formation and the second Bainite. The main discrepancies between the CCT diagram and experimental data are related to the formation of ferrite. The experimental data predicts a higher ferrite start temperature than the CCT diagram and, more significantly, a different position for the nose. According to the CCT diagram the nose occurs at cooling rates between 80°C/min and 90°C/min, whilst the experimental data suggests that it exists between the experimentally designated cooling rates of 30°C/min and 50°C/min. Predicting ferrite formation is important when attempting to optimise quenching processes. As previously stated the ferritic microstructure is detrimental to important material properties and whilst formation of small volume fractions can be tolerated, there exists a volume fraction that will causes properties to fall below specification levels. The CCT diagram can be considered conservative as ferrite formation is predicted at higher cooling rates than the experimental data,

but as relatively slow cooling rates are likely in thick section forgings, certainly below 80°C/min, failure maybe expected and costly optimisation work implemented unnecessarily.

Figures 6 and 7 compare thermocouple data against modelled results at various positions within the forging. Figure 6 compares 1/4T and 1/2T locations in the 331 mm section and figure 7 compares

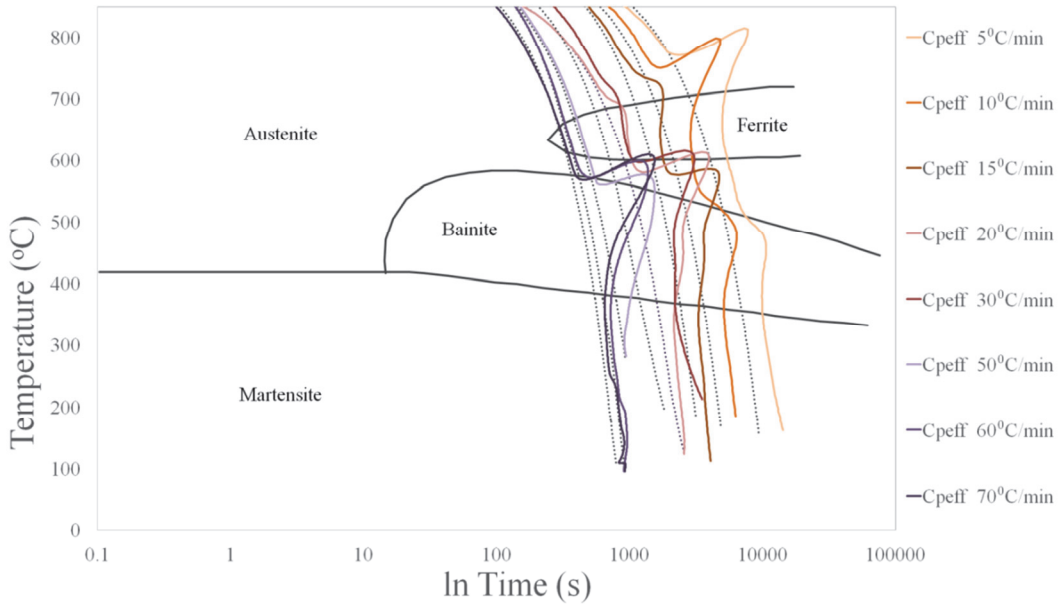

Fig. 3. *Plot of Cp_{eff} data with cooling curves and CCT diagram for SA508-3 adapted from Suzuki et al. (2001)*

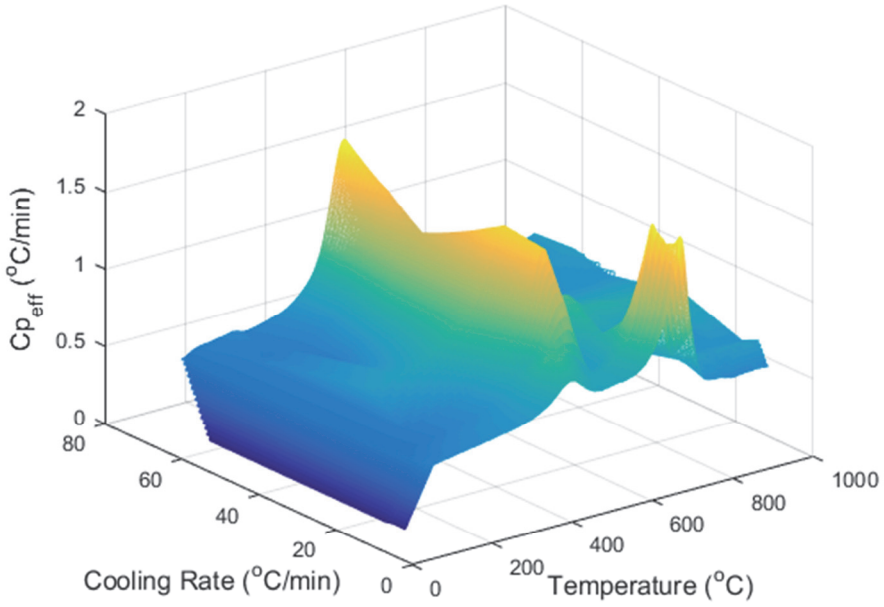

Fig. 4. *3D plot of Interpolated Cp_{eff} data*

Figure 4 is a plot of the interpolated Cp_{eff} data, at cooling rate intervals of 1°C/min. The figure clearly demonstrates how latent heat evolution changes as a function of cooling rate. Figure 5 shows the baseline data used in the FEM material file and UDR. Latent heat responses have been removed from the experimental data and demonstrates how specific heat capacity increases as a function of temperature.

the same locations in the thinner 200.5 mm section. First, considering the 1/2T locations, a reasonable agreement is seen between simulated and measured results. The modelled cooling curves initially match the thermocouple data but begin to deviate at temperatures below 800°C, predicting faster cooling rates than those measured. Although an exact fit

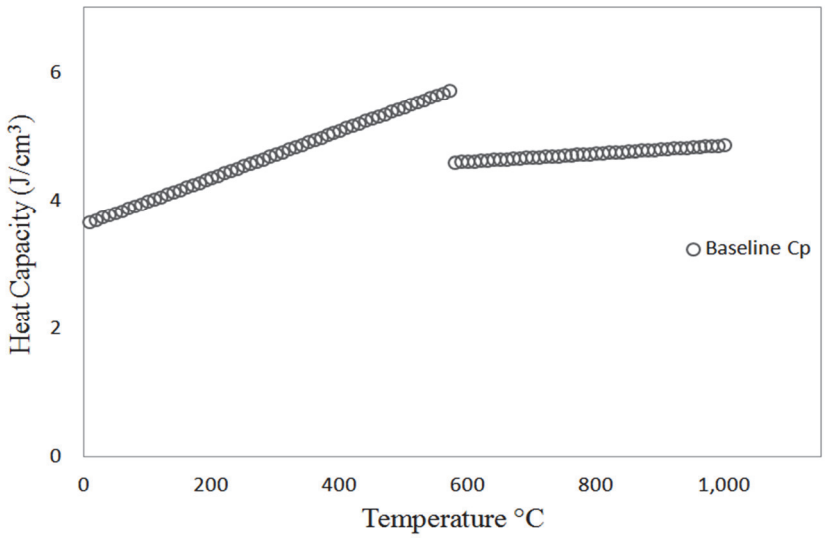

Fig. 5. *Baseline data incorporated in both FEM model and UDR. Experimental data was interpolated before and after transformations to generate the data.*

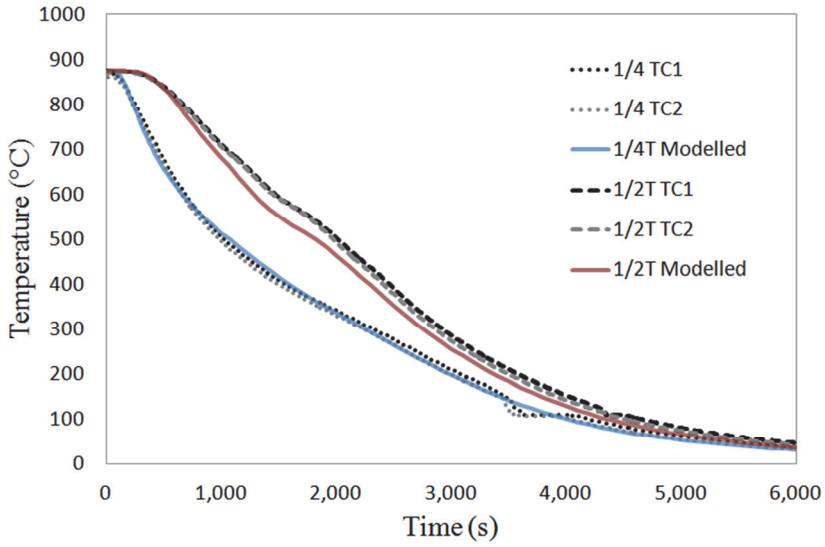

Fig. 6. *1/4T and 1/2T cooling curves the 331mm section, compared with simulated data.*

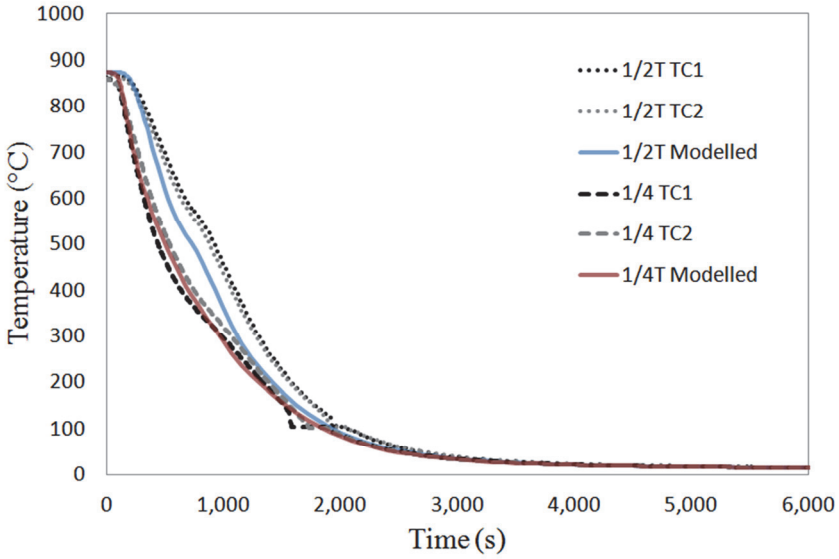

Fig. 7. *1/4T and 1/2T cooling curves the 200.5 mm section, compared with simulated data.*

was not achieved, the change in gradient between 500 and 600°C, associated with the latent heat from bainite formation, is replicated reasonably well and the overall trend of the cooling curve is matched. Considering the 1/4T positions, thermocouple data is more accurately reproduced by the model, with the best fit seen in the thinner 1/4T position.

The inability of the modelled data to achieve an exact fit to the experimental cooling curves can be attributed to aspects of the models construction. Firstly, there are questions regarding the accuracy of the experimental method used, for example the influence of austenite grain size on results. The prior austenite grain boundaries offer nucleation sites during quenching and hence influence the kinetics of reconstructive transformations. The final austenite grain size is subject to the initial microstructure of the sample, heating rate, austenitising time and temperature (Caballero et al., 2003; Pous-Romero et al., 2013). It is unknown if heating conditions successfully replicated the austenite grain size seen in production forgings, hence the experimental data may not have reproduced conditions seen in the full scale trial.

The modelling approach adopted in the construction of the UDR is another plausible reason for the small discrepancies seen. The designation of cooling rates is based upon the gradient of the time/temperature change between 830 and 800°C/min. The model assumes that the cooling rate calculated at each node remains constant throughout and therefore assigns the relevant Cp_{eff} data accordingly. If this assumption is not correct and the cooling rate changes, an incorrect data set maybe

called. The UDR is also reliant on interpolated data, the range of cooling rates examined may not be sufficient to interpolate and capture accurately the cooling rates seen in the thermocouple data. Further to this it is worth noting that the model is only representative of positions that have a maximum cooling rate of 70°C/min and a minimum cooling rate of 5°C/min. In the current model this point exists at between 60 and 70 mm deep, predicted cooling rates between the surface and these depths should be treated with caution. The 1/4T position of the thinner section is 50 mm from the surface and therefore within this window. The model is not currently capable of predicting accurate cooling rates at this location.

Finally, the manner in which quenching was represented may have contributed to the inaccuracies observed. The method of assigning time and temperature data as a boundary condition was suitable for replicating shallower depths but may have failed to represent the heat transfer characteristics required to reproduce cooling rates at the 1/2T. This may be due to the fact that the data from a single thermocouple was used to apply a uniform condition across a large surface area when, in reality, a more variable surface heat flux conditions was experienced.

These small issues aside, the fit produced by the model demonstrates the methodologies capability of reproducing general cooling rates in thick section forgings. What's more, the method demonstrated it was capable of achieving an excellent fit in key test locations.

Conclusion

The purpose of the paper was to accurately model temperature vs time data that incorporates the effects of phase transformations in thick sectioned nuclear forgings during quenching. This was achieved using values of specific heat containing the latent heat of transformation, known as the effective specific heat, produced using data obtained from differential scanning calorimetry, combined with finite element modelling. The following conclusions can be drawn:

- The transformation temperatures established for multiple cooling rates through DSC analysis correlated with data found in the literature, although discrepancies were also highlighted between the experimental results and the critical ferrite formation 'nose' predicted by a CCT diagram.
- The results of the model successfully reproduced cooling data recorded by thermocouples at 1/4T locations and attained a reasonable agreement with data recorded at the 1/2T locations.
- The small discrepancies at the 1/2T positions have been partially attributed to the modelling approach adopted, particularly the approach used to represent boundary conditions.
- The results demonstrate the capability of this modelling technique for reproducing cooling rates in key test location. In positions of significant depth a small amount of refinement is required to achieve the same level of model fidelity.

ACKNOWLEDGEMENTS

The authors would like to thank Dr. Daniel Cogswell for his contribution to the paper and Rolls-Royce Plc for their part in sponsoring the work. M. P. Howson also thanks the Engineering and Physical Science Research Council UK (EPSRC) for financial support through the EPSRC Centre for Doctoral Training in Advanced Metallic Systems.

REFERENCES

Al-Bermani, S. S., Davies, P. S., Chesman, C., Wynne, B. P., & Talamantes-Silva, J., 2015, Use of controlled heat treatment to predict mechanical properties in steel components, *Ironmaking & Steelmaking*, 43, 351-357.

American Society of Mecnahical Engineers (ASME)., 2013a, *ASME Boiler and Pressure Vessel Code*, Section II - Part A, 915-925.

American Society of Mecnahical Engineers (ASME)., 2013b, *ASME Boiler and Pressure Vessel Code*, Section II - Part D, 771-772.

Caballero, F. G., Capdevila, C., Andrés, C. G. D. E., 2003, An Attempt to Establish the Variables *That Most Directly Influence the Austenite Formation Process in Steels*, 43, 726-735.

Carlone, P., Palazzo, G. S., & Pasquino, R., 2010, Finite element analysis of the steel quenching process: Temperature field and solid–solid phase change, *Computers & Mathematics with Applications*, 59, 585-594.

Fernandes, F. M. B., Denis, S., Simon, A., 1985, Mathematical model coupling phase transformation and temperature evolution during quenching of steels, *Materials Science and Technology*, 1, 838-844.

Haverkamp, K. D., Forch, K., Piehl, K.-H., Witte, W., 1984, Effect of heat treatment and precipitation state on toughness of heavy section Mn-Mo-Ni-steel for nuclear power plants components, *Nuclear Engineering and Design*, 81, 207-217.

Howson, M. P., Wynne, B. P., Davies, P. S., Al-Bermani, S. S., Talamantes-Silva, J., 2016, A Comparison of Input Data Used to Represent Phase Transformations during the Quenching of a Large Nuclear Forging, *Key Engineering Materials*, 716, 555-565.

Jhajj, K. S., Slezak, S. R., Daun, K. J., 2015, Inferring the specific heat of an ultra high strength steel during the heating stage of hot forming die quenching, through inverse analysis, *Applied Thermal Engineering*, 83, 98-107.

Kim, J. T., Kwon, H. K., Chang, H. S., & Park, Y. W., 1997a, Improvement of impact toughness of the SA 508 class 3 steel for nuclear pressure vessel through steel-making and heat-treatment practices, *Nuclear Engineering and Design*, 174, 51-58.

Kim, J.-T., Kwon, H.-K., Kim, K.-C., Kim, J.-M., 1997b, Improved mechanical properties of the A 508 class 3 steel for nuclear pressure vessel through steelmaking, *Steel Forgings*, 2, 18-32.

Krielaart, G. P., Brakman, C. M., Van Der Zwaag, S., 1996, Analysis of phase transformation in Fe-C alloys using differential scanning calorimetry, *Journal of Materials Science*, 31, 1501-1508.

Liu, C. C., Xu, X. J., Liu, Z., 2003, A FEM modeling of quenching and tempering and its application in industrial engineering, *Finite Elements in Analysis and Design*, 39, 1053-1070.

Pan, J., Li, Y., Li, D., 2002, The application of computer simulation in the heat-treatment process of a large-scale bearing roller, *Journal of Materials Processing Technology*, 122, 241-248.

Pola, A., Gelfi, M., La Vecchia, G. M., 2013, Simulation and validation of spray quenching applied to heavy forgings, *Journal of Materials Processing Technology*, 213, 2247-2253.

Pous-Romero, H., Bhadeshia, H. K. D. H., 2014, Continuous Cooling Transformations in Nuclear Pressure Vessel Steels, *Metallurgical and Materials Transactions A*, 45, 4897-4906.

Pous-Romero, H., Lonardelli, I., Cogswell, D., Bhadeshia, H. K. D. H., 2013, Austenite grain growth in a nuclear pressure vessel steel, *Materials Science and Engineering: A*, 567, 72-79.

Rammerstorfer, F. G., Fischer, D. F., Mitter, W., Bathe, K. J., Snyder, M. D., 1981, On thermo-elastic-plastic analysis of heat-treatment processes including creep and phase changes, *Computers & Structures*, 13, 771-779.

Song, D. L., Gu, J. F., Zhang, W. M., LIU, Y., Pan, J., 2004, Numerical simulation on temperature and microstructure during quenching process of large-sized AISI P20 steel die blocks, *Trans. Mater. Heat Treatment*, 25, 740-745.

Suzuki, K., Kurihara, I., Sasaki, T., Koyoma, Y., Tanaka, Y., 2001, Application of high strength MnMoNi steel to pressure vessels for nuclear power plant, *Nuclear Engineering and Design*, 206, 261-277.

Tewkesbury, H., Stapley, A. G. F., Fryer, P. J., 2000, Modelling temperature distributions in cooling chocolate moulds, *Chemical Engineering Science*, 55, 3123–3132.

Woodard, P. R., Chandrasekar, S., Yang, H. T. Y., 1999, Analysis of temperature and microstructure in the quenching of steel cylinders, *Metallurgical and Materials Transactions B*, 30, 815-822.

MODELOWAMIE Z WYKORZYSTANIEM EFEKTYWNEJ POJEMNOŚCI CIEPLNEJ WPŁYWU PRZEMIANY FAZOWEJ NA PRĘDKOŚĆ CHŁODZENIA ODKUWKI DLA PRZEMYSŁU JĄDROWEGO

Streszczenie

Metodologię modelowania z wykorzystaniem efektywnej pojemności cieplnej wykorzystano do przewidywania wpływu ciepła przemiany na prędkość chłodzenia w masywnych częściach hartowanej odkuwki dla przemysłu jądrowego. Różnicowa kalorymetria skaningowa została zastosowana do pomiaru ciepła właściwego w funkcji temperatury (100 - 1000°C) i prędkości chłodzenia (5 and 70°C/min) z uwzględnieniem ciepła uwalnianego w czasie przemiany. Wyznaczone w taki sposób ciepło właściwe nazywane jest efektywnym. Uzyskane dane zaimplementowano poprzez procedurę użytkownika do programu metody elementów skończonych modelującego w pełnej skali obróbkę cieplną odkuwki posiadającej masywne części z przekrojem poprzecznym o grubości 200.5 i 331 mm. Uzyskano bardzo dobrą zgodność wyników z modelu i pomiaru za pomocą termopar umieszczonych w punktach testowych, w szczególności dla 0.25 i 0.5 grubości. Za przyczynę zaobserwowanych pewnych odchyłek wyników obliczeń od pomiarów uznano przyjęte założenia modelu, w szczególności metodę opisu warunków brzegowych.

Received: November 29, 2016
Received in a revised form: January 12, 2017
Accepted: February 5, 2018